Maximum T_c at the verge of a simultaneous order-disorder and lattice-softening transition in superconducting CaC_6

A. Gauzzi,[1,*] N. Bendiab,[1] M. d'Astuto,[1] B. Canny,[1] M. Calandra,[1] F. Mauri,[1] G. Loupias,[1] N. Emery,[2] C. Hérold,[2] P. Lagrange,[2] M. Hanfland,[3] and M. Mezouar[3]

[1]*Institut de Minéralogie et de Physique des Milieux Condensés, Université Pierre et Marie Curie Paris VI and CNRS, 75005 Paris, France*

[2]*Laboratoire de Chimie du Solide Minéral-UMR 7555 CNRS, Université Henri Poincaré Nancy I, 54506 Vandoeuvre-lès-Nancy, France*

[3]*European Synchrotron Radiation Facility, Boite Postale 220, 38043 Grenoble, France*

(Received 17 June 2008; published 5 August 2008)

In order to account for the large drop of superconducting critical temperature, T_c, and for the dramatic increase in residual resistivity, ϱ_0, previously reported in CaC_6 at $P_{cr} \approx 9$ GPa, we studied the room-temperature crystal structure of bulk CaC_6 samples as a function of pressure up to 13 GPa by means of synchrotron x-ray diffraction in diamond anvil cells. At P_{cr}, we found no change of the trigonal $R\bar{3}m$ space group symmetry, but a large increase in isothermal compressibility, κ, from -0.0082 GPa^{-1} to -0.0215 GPa^{-1}, accompanied by a large broadening of Bragg peaks. With both effects being reversible, it follows that superconductivity in CaC_6 is maximized at the verge of a peculiar order-disorder phase transition concomitant to a large lattice softening. Space group symmetry considerations supported by *ab initio* calculations of the relaxed structure within the density functional theory lead us to conclude that the disordered phase is presumably characterized by a random off-centering of the Ca atoms in the *ab* plane with respect to the C honeycomb layers.

DOI: 10.1103/PhysRevB.78.064506 PACS number(s): 74.70.Ad, 61.05.cp, 62.50.−p

I. INTRODUCTION

The properties of superconductors in presence of lattice instabilities have attracted a great deal of interest for a long time since the early evidence of enhanced critical temperatures, T_c, concomitant to soft phonon modes reported on a variety of systems such as simple elements,[1,2] A15 compounds,[3] transition metal carbides,[4] and borocarbides.[5,6] Recently, there was a renewed interest in the subject for soft modes were found to reflect electronic instabilities such as electronic phase separation in high-T_c cuprates,[7,8] charge density waves in layered dichalcogenides,[9,10] and strong electronic correlations in intercalated oxides such as Na_xCoO_2.[11–13] Thus, soft modes appear to be important for studying the stability of superconductivity and for maximizing T_c in complex systems.

Despite intense efforts, the field remains controversial, so it seems useful to focus on model systems displaying a clear link between microscopic Bardeen-Cooper-Schrieffer (BCS) parameters and mode softening. Here we study the lattice instability of the graphite intercalated compound (GIC) CaC_6 (Refs. 14 and 15) that has attracted a great deal of interest owing to the unusually high $T_c = 11.5$ K for GICs. Both experimental[16–18] and theoretical[19–21] studies point at a conventional BCS phonon-mediated pairing with a sizable electron-phonon coupling constant, $\lambda \approx 0.8$, and with *s*-wave gap symmetry. *Ab initio* calculations within the density functional theory (DFT) have put into evidence the dominant role of two phonons with in-plane Ca and out-of-plane C polarizations, respectively, in the pairing.[20,22,23] In addition, CaC_6 exhibits an interesting behavior under high pressure, P, as T_c first rapidly increases with pressure, until it reaches the record value of 15.1 K for GICs at 7.5 GPa, and then suddenly drops to ≈ 5 K at $P_{cr} \approx 9$ GPa.[24] This drop is accompanied by a dramatic increase in the residual resistivity, ϱ_0, and by an anomalous softening (hardening) of the above Ca (C) mode.[24] Indeed, a pressure-induced vanishing of the Ca mode has been predicted[22,23,25] and possible high-pressure structures have been calculated.[26,27] However, no high-pressure structural data are available yet so the origin of the structural instability and of the corresponding change of transport properties remains to be determined. In order to address these issues, in this work we studied the room-temperature crystal structure of CaC_6 at high pressures up to 13 GPa. At P_{cr}, we found a jump of the isothermal compressibility concomitant to a large Bragg peak broadening. This unveils a unique order-disorder phase transition concomitant to a lattice softening, which accounts for the above T_c reduction and phonon anomalies.

II. EXPERIMENT

The experiment was carried out at the high-pressure diffraction beamline ID9 of the ESRF. A high-quality ≈ 1 mm size bulk sample of CaC_6 was prepared from a platelet of highly oriented pyrolithic graphite, as described elsewhere.[28] A few $\approx 50-100$ μm pieces were mounted in two diamond anvil cells (DAC) in the usual opposite anvil configuration. The cells were subsequently charged with high purity helium (sample 1) and argon (sample 2) used as pressure-transmitting media. Due to the reactivity of CaC_6, the procedure was carried out in a high-purity dry box, where the cells were sealed under an initial gas pressure of 0.1 GPa.

The diffractograms were taken in the Debye-Scherrer geometry suitable for the above DAC configuration using a wavelength $\lambda = 0.4133$ Å. The diffracted beam was collected within a maximum diffraction angle $2\vartheta_{max} = 25°$ by an image plate. Owing to the small diameter of the stainless steel gasket (150 μm), the beam spot size was reduced down to

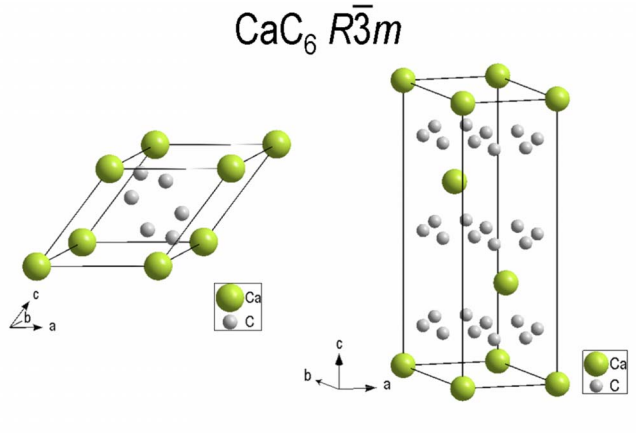

FIG. 1. (Color online) Rhombohedral (left) and hexagonal (right) unit cells of $R\bar{3}m$ CaC_6, according to Table I. The latter unit cell enables a better visualization of the stacking of the Ca and C layers; the corresponding volume is three times larger than that of the former unit cell (Ref. 28).

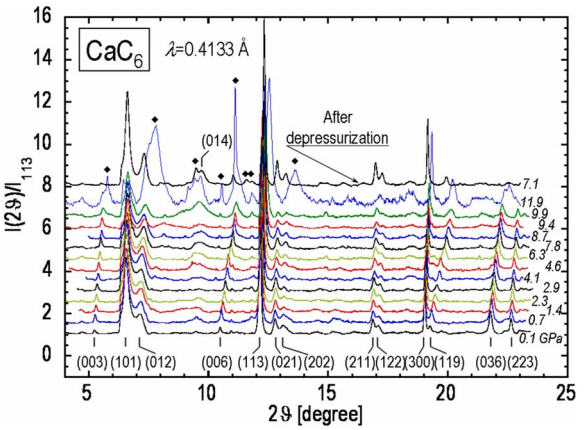

FIG. 2. (Color online) Representative diffractograms of Sample 1 at different pressures upon pressurization and depressurization. Intensities are normalized to the maximum intensity of the strongest (113) peak. Bragg indices refer to the hexagonal unit cell of Fig. 1. Diamonds mark unindexed peaks and additional broad features appearing above 9 GPa (see text).

40 μm for $P \leq 10$ GPa. At higher pressures, this size was further reduced to 20 μm due to the shrinkage of the cell. For each pattern, the pressure value was determined from the emission line of a ruby crystal. To maximize the number of reflections detected, the DAC was spindled within an angle of $\pm 3°$ with respect to the incident beam direction. This is especially important in our case, as the layered structure of CaC_6 is expected to induce a preferential orientation of the graphene layers perpendicular to the incident beam. For both samples, no significant amount of secondary phases was detected in the sample regions probed by the x-ray beam. This enabled us to reliably refine the unit cell up to 13 GPa, as described below.

III. UNIT-CELL REFINEMENT

Sample 1 gave a larger signal-to-background ratio, so the analysis below mainly refers to this sample. More than hundred diffractograms were taken on sample 1 by progressively increasing pressure from 0.1 up to 13 GPa and upon depressurization. Representative diffractograms are shown in Fig. 2. All of the main Bragg peaks are found to match those of the trigonal $R\bar{3}m$ phase (see Fig. 1), in agreement with the report by Emery *et al.*[28] Two unit-cell choices corresponding to either rhombohedral or hexagonal axes are possible (see Table I, Ref. [29] and Fig. 1). The indexation adopted for Fig. 2 corresponds to the latter choice, which enables to better visualize the crystal structure as an alternate stacking of graphene and Ca layers (see Fig. 1). The additional features appearing above 9 GPa are to be discussed later.

The indexation of Fig. 2 shows that despite the expected preferential orientation of the sample, reflections with various combinations of h, k, and l indices are present. This might be due to the folding of the CaC_6 flakes during sample manipulation. About thirty diffractograms in the 0.1–13 GPa range were selected for the unit cell refinement. For the $P \leq 10$ GPa data, we typically used as many as 12–15 Bragg reflections. This number reduces to eight at higher pressures because of the weaker signal and the appearance of additional broad features to be discussed later. The result of the refinement and the equation of state are shown in Fig. 3. Thanks to the presence of strong (300), (113), (003), and

TABLE I. Nuclear structure of the trigonal phase of CaC_6 (space group $R\bar{3}m$) in the rhombohedral and hexagonal axes (Ref. 28). The room-temperature lattice parameters are $a=5.17$ Å and $\alpha=49.55°$ in the former case, and $a=b=4.33$ Å and $c=13.57$ Å in the latter case. Atomic coordinates x, y, z are in reduced lattice units; SOF denotes the site occupancy factor. Note that the x coordinate of the C site is not set by symmetry (see also Ref. 29). The regular C honeycomb structure corresponds to $x=1/6$ or $x=1/3$ for the rhombohedral and hexagonal axes, respectively.

	Atomic site	Wyckoff position	Site symm.	x	y	z	SOF
Rhombohedral	Ca	$1a$	$\bar{3}m$	0	0	0	1
axes	C	$6g$	.2	x	$\bar{x}$	1/2	1
Hexagonal	Ca	$3a$	$\bar{3}m$	0	0	0	1
axes	C	$18g$	.2	x	0	1/2	1

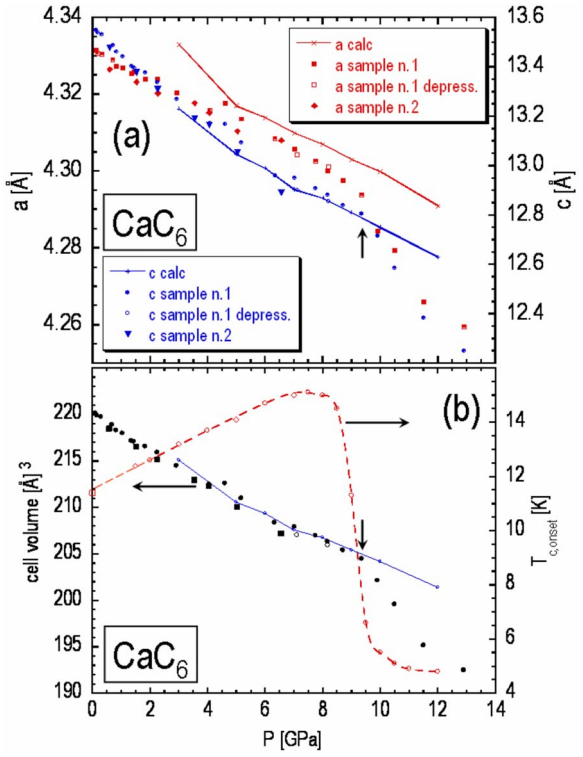

FIG. 3. (Color online) (a) Experimental (symbols) and calculated (solid lines) pressure dependence of the hexagonal a and c cell parameters. (b) pressure dependence of the unit cell volume corresponding to the data (symbols) and calculations (solid line) of panel (a). The onset T_c vs P data from Ref. 24 are also reported to show that the T_c drop coincides with the kink of the equation of state at 9 GPa, marked by vertical arrows. The broken line is a guide to the eye.

(006) peaks corresponding to independent Bragg planes, the accuracy obtained for the a and c parameters is as good as $\pm 0.001-0.002$ and $\pm 0.002-0.004$ Å, respectively. Good refinements were obtained also using the data of samples 1 and 2 upon depressurization and pressurization, respectively. The comparison of the three data sets shows their reproducibility within the experimental error and no hysteresis is found upon depressurization.

IV. EXPERIMENTAL AND THEORETICAL EQUATION OF STATE FOR CaC_6

A summary of the results obtained from the unit-cell refinement described above is shown in Fig. 3. One notes that both a and c parameters decrease roughly linearly with pressure down to 9 GPa. In this range, a linear regression yields the following isothermal compressibility coefficients: $da/dP=-0.0038$ Å/GPa; $dc/dP=-0.081$ Å/GPa. Hence, the c-axis compressibility is about twenty times larger than the in-plane one, as expected considering the layered structure. The corresponding isothermal compressibility is $\kappa = (1/V_{9\ \mathrm{GPa}})dV/dP=-0.0082\ \mathrm{GPa}^{-1}$. The above values and the large anisotropy are consistent with previous studies on graphite[30] and graphite intercalated compounds with same composition and similar crystal structure such as LiC_6.[31] In order to study in more detail the pressure-induced structural changes, the relaxed structure was calculated as a function of pressure up to 12 GPa using the ESPRESSO DFT code,[33] as described elsewhere.[20,22] In Fig. 3, the results of the calculations are compared to the experimental data. For $P \lesssim 9$ GPa, it is noted a good agreement for both a and c parameters, except a slight overestimation of the former.

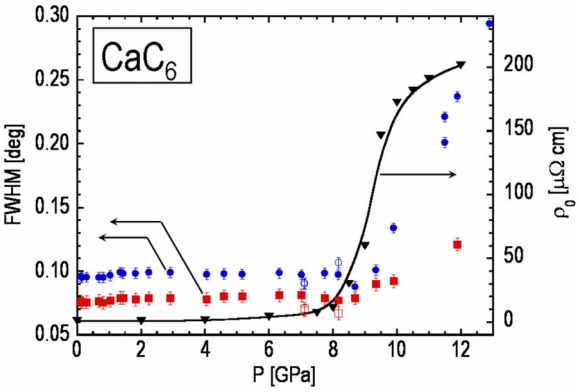

FIG. 4. (Color online) Pressure dependence of the full width at half maximum (FWHM) of the (113) (circles) and (300) (squares) peaks. Open symbols refer to data after depressurization. The dependence of the residual resistivity, ϱ_0 (triangles), taken from Ref. 24 is also shown for comparison (the line is a guide to the eye). Error bars are smaller than symbols when not visible.

V. EVIDENCE OF ORDER-DISORDER AND LATTICE-SOFTENING TRANSITION AT 9 GPa

Notable feature of the experimental equation of state of Fig. 3 is a kink at 9 GPa corresponding to a jump of κ, evidence of a second-order phase transition. The discrepancy between experiment and calculations in the $P \gtrsim 9$ GPa range is due to the fact that the relaxed structure was calculated using the rhombohedral cell of Fig. 1 for all pressure values. In fact, the kink indicates that this structure is unstable above 9 GPa, as will be discussed later. A linear fit of the experimental data in the $P \gtrsim 9$ GPa region yields $\kappa = (1/V_{9\ \mathrm{GPa}})dV/dP=-0.0215\ \mathrm{GPa}^{-1}$. Thus, the high-pressure structure is almost three times softer than the low-pressure one.

In order to unveil the origin of this jump of κ, we notice the following: (1) The analysis of the diffraction data of Fig. 2 in the pressure range near the kink in the equation of state indicates no change of space group symmetry as no sizable new peaks are detected. (2) The kink is concomitant to a dramatic peak broadening, which turns out to be fully reversible upon depressurization (see Figs. 4 and 5). Result (1) rules out the formation of new high-pressure phases such as those predicted by the *ab initio* calculations of Refs. 26 and 27. Also, we should rule out the possibility of pressure-induced staging transitions, which are known to occur in other GICs at $P \sim 0.1$ GPa,[32] for these transitions would lead to a change of c-axis parameter. On the other hand, result (2) suggests that the second-order phase transition at 9 GPa is associated with an incipient amorphous phase or the formation of pressure-induced disorder.

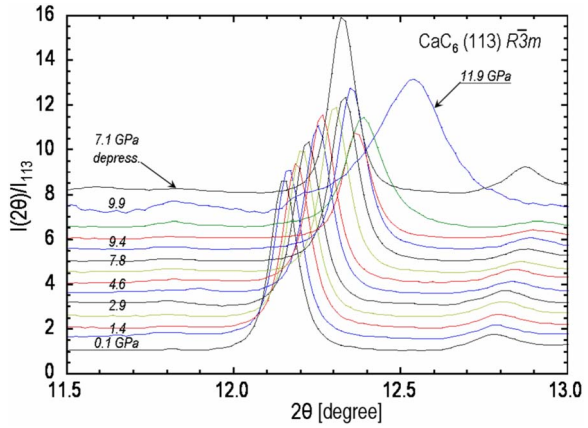

FIG. 5. (Color online) Evolution of the (113) peak profile upon pressure. Note the recovery of the pristine width and maximum intensity upon depressurization.

An important hint as to the structural changes occurring at 9 GPa is obtained by using symmetry arguments supported by *ab initio* calculations of the relaxed structure. We recall that the only free parameter of the $R\bar{3}m$ structure is the in-plane coordinate, x, of the C site in the *ab* plane of the hexagonal cell (see Table I and Ref. 29). As mentioned in the legend of Table I, the regular honeycomb structure of the C layers corresponds to $x=1/3$. Different x values would correspond to a deformed structure within the *ab* plane. It is unlikely that pressure would induce this type of deformation for our *ab initio* calculations of the relaxed structure, used to compute the pressure-dependent unit-cell parameters of Fig. 3, show that the structure is extremely rigid within the *ab* plane. Therefore, since we find no evidence of change of space group symmetry at the kink, no changes of the crystal structure are consistent with our data. On the other hand, recent *ab initio* studies[20,23] suggest that the off-center displacement of the Ca atoms in the *ab* plane with respect to the C honeycomb structure requires a modest amount of energy, as shown by the soft phonon mode associated with this displacement. Furthermore, the above studies predict the enhanced softening of this mode with pressure,[23] in full agreement with our previous report of anomalous softening of this mode[24] and with our present observation of abrupt lattice softening at 9 GPa. In summary, the above considerations point at a progressive pressure-induced flattening of the potential of the Ca atoms relative to their off-center displacement in the *ab*-plane. We conclude that at some point, any position of the Ca atoms within the *ab* plane between adjacent C layers should become energetically equivalent. Owing to the symmetry constraint discussed previously, only random displacements of the Ca atoms are allowed, in full agreement with our experimental observation of Bragg peak broadening concomitant to the kink at 9 GPa. We conclude that at 9 GPa, an order-disorder transition of the Ca sublattice occurs.

This disordering mechanism is consistent with our previous observation of anomalous hardening of the out-of-plane C mode and of bad metallic properties with high residual resistivity values and flat resistivity curves above 8 GPa.[24] It is also consistent with the above *ab initio* studies on the high-pressure stability of CaC_6,[26,27] which predict the formation of lower-symmetry variants of the pristine $R\bar{3}m$ structure such as *Cm*. Indeed, these structures are characterized by off-centered Ca atoms with respect to the C honeycomb layers and by a buckling of these layers. Apparently, our results indicate that nature prefers a disordered arrangement of the intercalant Ca atoms in the *ab* plane rather than lowering the pristine $R\bar{3}m$ space group symmetry. Though, high-resolution data may enable to detect minor distortions (if any) of the $R\bar{3}m$ structure. *Mutatis mutandis*, an instability of the intercalant sublattice under high pressure was recently reported also in the graphite intercalated compound CsC_8.[34]

Finally, we should discuss the minor non-reversible changes of the diffraction patterns observed upon depressurization. We have found (see also Fig. 2) that these changes only concern the relative intensity of some peaks. Specifically, the doublet at $2\vartheta \approx 9.5°$ [the higher angle peak of the doublet being the (104) reflection] becomes stronger, whilst the (003), (036), and (223) peaks almost vanish. The following phenomena may account for these changes: (1) a pressure-induced texture change, which typically is irreversible; (2) a partial and irreversible transformation of the pristine $R\bar{3}m$ phase into the hexagonal $P6_3/mmc$ one, whose energy is only slightly larger.[22] Indeed, the diffraction patterns of the two phases are similar but the peak intensities are different. For example, the (002) reflection of the $P6_3/mmc$ phase, which corresponds to the (003) one of the $R\bar{3}m$ phase, is weak, in agreement with our observation. High-resolution data on single crystals would help to verify the above scenarios.

VI. CONCLUSIONS

In conclusion, by means of synchrotron x-ray diffraction under high pressure, we have found that the T_c drop and the dramatic increase in residual resistivity previously reported in superconducting CaC_6 at ≈ 9 GPa are caused by an order-disorder phase transition with no change of the $R\bar{3}m$ space group symmetry of the ambient pressure phase. This transition is found to be concomitant to a nearly three-time increase in isothermal compressibility. Space group symmetry arguments supported by the above lattice softening and by *ab initio* calculations suggest that the disorder consists of random off-center displacements of the Ca atoms in the *ab* plane with respect to the C honeycomb layers. This is the case of superconductor-superconductor phase transition driven by a simultaneous order-disorder and lattice-softening transition. We argue that this conclusion provides a clear framework for understanding the microscopic mechanisms limiting T_c in BCS superconductors.

ACKNOWLEDGMENTS

We gratefully acknowledge the ESRF for support (experiment n. HS3120) and thank M. Gauthier, Y. Le Godec, A. Polian, and A. Shukla for their valuable comments and suggestions and Y. Grin, K.A. Mueller, U. Schwarz, and H. Takagi for stimulating discussions.

*andrea.gauzzi@upmc.fr

[1] F. Mauri, O. Zakharov, S. de Gironcoli, S. G. Louie, and M. L. Cohen, Phys. Rev. Lett. **77**, 1151 (1996).
[2] G. Profeta, C. Franchini, N. N. Lathiotakis, A. Floris, A. Sanna, M. A. L. Marques, M. Luders, S. Massidda, E. K. U. Gross, and A. Continenza, Phys. Rev. Lett. **96**, 047003 (2006).
[3] L. R. Testardi, Rev. Mod. Phys. **47**, 637 (1975).
[4] H. G. Smith, Phys. Rev. Lett. **29**, 353 (1972).
[5] P. Dervenagas, M. Bullock, J. Zarestky, P. Canfield, B. K. Cho, B. Harmon, A. I. Goldman, and C. Stassis, Phys. Rev. B **52**, R9839 (1995).
[6] I. K. Yanson, V. V. Fisun, A. G. M. Jansen, P. Wyder, P. C. Canfield, B. K. Cho, C. V. Tomy, and D. M. Paul, Phys. Rev. Lett. **78**, 935 (1997).
[7] M. d'Astuto, P. K. Mang, P. Giura, A. Shukla, P. Ghigna, A. Mirone, M. Braden, M. Greven, M. Krisch, and F. Sette, Phys. Rev. Lett. **88**, 167002 (2002).
[8] D. Reznik, L. Pintschovius, M. Ito, M. Sato, H. Goka, M. Fujita, K. Yamada, G. D. Gu, and J. M. Tranquada, Nature (London) **440**, 1170 (2006).
[9] J. C. Tsang, J. E. Smith, Jr., and M. W. Shafer, Phys. Rev. Lett. **37**, 1407 (1976).
[10] T. E. Kidd, T. Miller, M. Y. Chou, and T.-C. Chiang, Phys. Rev. Lett. **88**, 226402 (2002).
[11] P. Zhang, W. Luo, V. H. Crespi, M. L. Cohen, and S. G. Louie, Phys. Rev. B **70**, 085108 (2004).
[12] J.-P. Rueff, M. Calandra, M. d'Astuto, Ph. Leininger, A. Shukla, A. Bossak, M. Krisch, H. Ishii, Y. Cai, P. Badica, T. Sasaki, K. Yamada, and K. Togano, Phys. Rev. B **74**, 020504(R) (2006).
[13] Q. Zhang, M. An, S. Yuan, Y. Wu, D. Wu, J. Luo, N. Wang, W. Bao, and Y. Wang, Phys. Rev. B **77**, 045110 (2008).
[14] Th. E. Weller, M. Ellerby, S. S. Saxena, R. P. Smith, and N. T. Skipper, Nat. Phys. **1**, 39 (2005).
[15] N. Emery, C. Hérold, M. d'Astuto, V. Garcia, Ch. Bellin, J.-F. Marêché, P. Lagrange, and G. Loupias, Phys. Rev. Lett. **95**, 087003 (2005).
[16] G. Lamura, M. Aurino, G. Cifariello, E. Di Gennaro, A. Andreone, N. Emery, C. Hrold, J. F. March, and P. Lagrange, Phys. Rev. Lett. **96**, 107008 (2006).
[17] N. Bergeal, V. Dubost, Y. Noat, W. Sacks, D. Roditchev, N. Emery, C. Herold, J. F. Mareche, P. Lagrange, and G. Loupias, Phys. Rev. Lett. **97**, 077003 (2006).
[18] J. S. Kim, R. K. Kremer, L. Boeri, and F. S. Razavi, Phys. Rev. Lett. **96**, 217002 (2006).
[19] G. Csányi, P. B. Littlewood, A. H. Nevidomskyy, C. J. Pickard, and B. D. Simons, Nat. Phys. **1**, 42 (2005).
[20] M. Calandra and F. Mauri, Phys. Rev. Lett. **95**, 237002 (2005).
[21] I. I. Mazin, Phys. Rev. Lett. **95**, 227001 (2005).
[22] M. Calandra and F. Mauri, Phys. Rev. B **74**, 094507 (2006).
[23] L. Zhang, Y. Xie, T. Cui, Y. Li, Z. He, Y. Ma, and G. Zou, Phys. Rev. B **74**, 184519 (2006).
[24] A. Gauzzi, S. Takashima, N. Takeshita, C. Terakura, H. Takagi, N. Emery, C. Hérold, P. Lagrange, and G. Loupias, Phys. Rev. Lett. **98**, 067002 (2007).
[25] J. S. Kim, L. Boeri, R. K. Kremer, and F. S. Razavi, Phys. Rev. B **74**, 214513 (2006).
[26] G. Csányi, Ch. J. Pickard, B. D. Simons, and R. J. Needs, Phys. Rev. B **75**, 085432 (2007).
[27] Y. Li, L. J. Zhang, T. Cui, Y. H. Liu, Y. M. Ma, and G. T. Zou, Chin. Phys. Lett. **24**, 1668 (2007).
[28] N. Emery, C. Hérold, and Ph. Lagrange, J. Solid State Chem. **178**, 2947 (2005).
[29] *International Tables of Crystallography*, Space-Group Symmetry Vol. I, edited by T. Hahn (Springer-Verlag, Heidelberg, 2005).
[30] M. S. Dresselhaus and G. Dresselhaus, Adv. Phys. **30**, 139 (1981).
[31] R. Clarke and C. Uher, Adv. Phys. **33**, 469 (1984).
[32] J. E. Fischer and H. J. Kim, Phys. Rev. B **35**, 6826 (1987).
[33] S. Baroni, S. de Gironcoli, A. Dal Corso, and P. Giannozzi, Rev. Mod. Phys. **73**, 515 (2001); See also http://www.pwscf.org
[34] N. Rey, P. Toulemonde, D. Machon, L. Duclaux, S. Le Floch, V. Pischedda, J. P. Itié, A. M. Flank, P. Lagarde, W. A. Crichton, M. Mezouar, T. Strassle, D. Sheptyakov, G. Montagnac, and A. San-Miguel, Phys. Rev. B **77**, 125433 (2008).